Mettl3-mediated m^{6}A RNA methylation regulates osteolysis induced by titanium particles

XIAOXUAN LIN[1*], YANG YANG[1*], YAOHONG HUANG[1], E LI[2], XIUMEI ZHUANG[3], ZHENGCHUAN ZHANG[1], RUOGU XU[1], XIAOLIN YU[1] and FEILONG DENG[1]

[1]Department of Oral Implantology, Hospital of Stomatology, Guanghua School of Stomatology, Sun Yat-sen University, Guangzhou, Guangdong 510055; [2]Department of Stomatology, Zhuhai Center for Maternal and Child Healthcare, Zhuhai Women and Children's Hospital, Zhuhai, Guangdong 519000; [3]Department of Stomatology, Sun Yat-sen Memorial Hospital, Sun Yat-sen University, Guangzhou, Guangdong 510000, P.R. China

Received August 11, 2023; Accepted November 24, 2023

DOI: 10.3892/mmr.2024.13160

Abstract. Peri-prosthetic osteolysis (PPO) induced by wear particles is considered the primary cause of titanium prosthesis failure and revision surgery. The specific molecular mechanisms involve titanium particles inducing multiple intracellular pathways, which impact disease prevention and the targeted therapy of PPO. Notably, N6-methyladenosine (m^{6}A) serves critical roles in epigenetic regulation, particularly in bone metabolism and inflammatory responses. Thus, the present study aimed to determine the role of RNA methylation in titanium particle-induced osteolysis. Results of reverse transcription-quantitative PCR (RT-qPCR), western blotting, ELISA and RNA dot blot assays revealed that titanium particles induced osteogenic inhibition and proinflammatory responses, accompanied by the reduced expression of methyltransferase-like (Mettl) 3, a key component of m^{6}A methyltransferase. Specific lentiviruses vectors were employed for Mettl3 knockdown and overexpression experiments. RT-qPCR, western blotting and ELISA revealed that the knockdown of Mettl3 induced osteogenic inhibition and proinflammatory responses comparable with that induced by titanium particle, while Mettl3 overexpression attenuated titanium particle-induced cellular reactions. Methylated RNA immunoprecipitation-qPCR results revealed that titanium particles mediated the methylation of two inhibitory molecules, namely Smad7 and SMAD specific E3 ubiquitin protein ligase 1, via Mettl3 in bone morphogenetic protein signaling, leading to osteogenic inhibition. Furthermore, titanium particles induced activation of the nucleotide binding oligomerization domain 1 signaling pathway through methylation regulation, and the subsequent activation of the MAPK and NF-κB pathways. Collectively, the results of the present study indicated that titanium particles utilized Mettl3 as an upstream regulatory molecule to induce osteogenic inhibition and inflammatory responses. Thus, the present study may provide novel insights into potential therapeutic targets for aseptic loosening in titanium prostheses.

Correspondence to: Dr Xiaolin Yu or Dr Feilong Deng, Department of Oral Implantology, Hospital of Stomatology, Guanghua School of Stomatology, Sun Yat-sen University, 56 Lingyuanxilu Street, Guangzhou, Guangdong 510055, P.R. China
E-mail: yuxlin3@mail.sysu.edu.cn
E-mail: dengfl@mail.sysu.edu.cn

*Contributed equally

Key words: osteolysis, aseptic loosening, titanium particles, methyltransferase-like 3, N6-methyladenosine RNA methylation, epigenetic regulation

Introduction

Titanium prostheses exhibit widespread uses in the clinic, including joint replacements and dental implants. However, in the majority of clinical cases, patients may experience ongoing inflammation in the absence of infection, which may lead to peri-prosthetic osteolysis (PPO) and subsequent aseptic loosening (1-4). The results of numerous studies have indicated that titanium implants undergo corrosion via various mechanisms inside the human body, including mechanical wear, biological activity and electrochemical processes (5-7). The aforementioned corrosion may cause gradual deterioration of the titanium implant; thus, impacting the structural integrity. In addition, the results of previous studies have demonstrated that the major cause of aseptic loosening is the gradual accumulation of wear particles around the titanium implant (8-10). Following 10 years of follow up, this phenomenon resulted in an implant failure rate of 32-62% following orthopedic surgery (11,12). For dental implants, unexplained mucosal inflammation impacts 43% of implants, and ongoing bone loss occurs in 6-29% of cases (13,14).

Numerous studies have focused on the molecular and cellular interactions between humans and wear particles (15,16). Previous studies have defined aseptic loosening as an immune-mediated biological complication (2,17-19). However, the complex interplay among the innate or adaptive immune response, the skeletal system and wear particles remains to be fully understood. Previous studies have revealed

that the released particles may induce a cascade of biological effects, including potent proinflammatory immune responses, suppression of osteoblast function and activation of osteoclasts, leading to peri-implant bone loss (20-25). Thus, research has focused on the specific molecular mechanisms and potential targeted drugs for use in the clinic. Previous studies have revealed numerous inhibitors that exert protective effects on titanium particle-induced bone loss, and multiple associated downstream signaling pathways, such as the MAPK, NF-κB, GSK-3β/β-catenin and TGF-β pathways (10,22,26-31). Notably, multiple pathways are simultaneously activated by titanium particles. Thus, previous studies that focused on a single target or downstream pathway were unsuccessful in uncovering the specific mechanisms, and therapies that target single pathways to attenuate particle-induced osteogenic inhibition or inflammatory responses are limited (30,32,33).

N6-methyladenosine (m^6A), a dynamic methylation at the N6 site of adenosine, is the most common post-transcriptional RNA modification. As an epigenetic regulator, it regulates numerous biological processes through mediating RNA metabolism, including degradation and translation (34-36). The methyltransferase-like (Mettl)3/Mettl14 catalytic heterodimer serves a role in the methylation of m^6A. The process of demethylation is implemented by demethylases, including ALKB homolog 5 and fat mass and obesity-associated protein. This specific modification is recognized and bound by m^6A reader proteins, mainly from YT521-B homology (YTH)-domain family proteins (37-41). Previous studies have revealed the association between m^6A modifications and bone metabolism. RNA methylation serves a significant role in regulating bone homeostasis. Notably, Mettl3 and/or Mettl14 deficiency may disrupt the proliferation and differentiation of stem cells, such as bone marrow mesenchymal stem cells, causing bone disorders, such as osteoporosis (42-46). In addition, previous studies have demonstrated that post-transcriptional modification via changes in expression of methyltransferases, demethylases or reader proteins concurrently regulated multiple downstream pathways, achieving regulation in diverse cellular reactions (46,47).

As m^6A modifications are essential in bone homeostasis (48), the present study aimed to explore the role of m^6A modification in titanium particle-induced osteolysis. In addition, the present study aimed to provide novel insights into potential therapeutic targets for aseptic loosening. It was hypothesized that titanium particles may utilize RNA methylation as a form of upstream regulation to induce multiple subsequent pathways; thus, causing osteogenic inhibition and inflammatory responses.

Materials and methods

Titanium particle preparation. The titanium particles used in the present study were obtained from Alfa Aesar; Thermo Fisher Scientific, Inc. and prepared as previously described (10,22,29). Briefly, the particles were incubated at 180˚C for 12 h, and subsequently immersed in 75% ethanol at room temperature for 48 h to eliminate endotoxins. Endotoxin levels in particles were detected using a Limulus assay kit (Xiamen Bioendo Technology Co., Ltd.) to ensure that endotoxin levels were <0.02 EU/ml.

Cell culture and treatment. The cells used in the present study were cultured at 37˚C with 5% CO_2. The murine osteoblast cell line, MC3T3-E1 (iCell Bioscience, Inc.) was cultured in α-minimum essential medium (Gibco; Thermo Fisher Scientific, Inc.) with 10% FBS (Gibco; Thermo Fisher Scientific, Inc.) and 100 U/ml penicillin/streptomycin (Gibco; Thermo Fisher Scientific, Inc.). For osteogenic differentiation, cells were cultured in the aforementioned growth medium with the addition of 50 μg/ml ascorbic acid (Sigma-Aldrich; Merck KGaA) and 10 mM β-glycerophosphate (Sigma-Aldrich; Merck KGaA). The prepared titanium particles were used at a concentration of 100 μg/ml. For titanium particle treatment groups, particles were cocultured with osteogenic induction medium to figure out the effect of titanium particles on osteoblasts in an osteogenic environment (10,22).

The RAW264.7 mouse macrophage cell line was purchased from American Type Culture Collection and cultured in DMEM (Gibco; Thermo Fisher Scientific, Inc.) with 10% FBS and 100 U/ml penicillin/streptomycin (Gibco; Thermo Fisher Scientific, Inc.). The supernatants of osteoblast cells with different treatments, including titanium particle treatment and the knockdown or overexpression of the Mettl3 gene, were harvested and then centrifuged at 500 x g at room temperature for 5 min to remove cell debris or titanium particles. Subsequently, the supernatant was mixed with culture medium at a ratio of 1:1 (conditioned medium) and then RAW264.7 cells were cultured in conditioned medium for the detection of osteoclastic differentiation. Cells cultured in growth medium were used as the negative control (NC), while cells treated with 50 ng/ml recombinant murine receptor activator of NF-κB ligand (RANKL; PeproTech, Inc.) were used as the positive control. The samples were collected at 2 and 3 days for reverse transcription-quantitative PCR (RT-qPCR) and western blotting, respectively.

For nucleotide binding oligomerization domain (NOD)1 pathway inhibition experiments, osteoblast cells were pretreated with 30 μM ML130 (MedChemExpress) and 10 μM WEHI-345 (Abmole Bioscience Inc.) at 37˚C for 2 h (49,50).

Transmission electron microscopy (TEM). Following co-culture with titanium particles for 24 h, osteoblast cells were collected and fixed with 2.5% glutaraldehyde in PBS at 4˚C for 1 h. No stain was used as the stain would highlight various intracellular structures. Cells were fixed with 1% osmium tetroxide in H_2O for 2 h, followed by sequential dehydration with a graded ethanol series. Samples were embedded in epoxy resin at 60˚C for 12 h, cut into 70-90-nm ultrathin sections and subsequently observed using a JEM-1200EX electron microscope (JEOL, Ltd.).

RT-qPCR. Total RNA was extracted from cells using TRIzol® reagent (Invitrogen; Thermo Fisher Scientific, Inc.). cDNA was synthesized using total RNA and HiScript III RT SuperMix (Vazyme Biotech Co., Ltd.) at 37˚C for 15 h and then 85˚C for 5 sec. ChamQ Universal SYBR qPCR Master Mix (Vazyme Biotech Co., Ltd.) and a Light Cycler 480 (Roche Diagnostics GmbH) were employed to amplify cDNA. The initial denaturation condition was 95˚C for 10 sec. The thermocycling (40 cycles) conditions were as follows: 95˚C for 10 sec and 60˚C for 30 sec. mRNA levels were quantified using the

$2^{-\Delta\Delta Cq}$ method and normalized to the internal reference gene GAPDH (51). The specific primers are listed in Table SI.

Western blotting. Following rinsing three times with PBS, cells were lysed using RIPA buffer (Beyotime Institute of Biotechnology) supplemented with protease and phosphatase inhibitors (CoWin Biosciences). Cell homogenates were obtained and centrifuged at 14,000 x g for 20 min at 4˚C. The cell supernatant was obtained and a BCA protein assay kit (CoWin Biosciences) was used to determine the concentration of total proteins. Samples were subsequently incubated at 95˚C for 10 min in SDS-PAGE sample loading buffer (Beyotime Institute of Biotechnology) for denaturation. 20 μg total protein samples were separated via 4-12% SDS-polyacrylamide gel electrophoresis and transferred to PVDF membranes (MilliporeSigma). Membranes were blocked in 5% skimmed milk powder supplemented with 1X TBS-1‰ Tween-20 (TBS-T) at room temperature for 1 h, and subsequently incubated with primary antibodies at 4˚C for 12 h. All primary antibodies are listed in Table SII. Following rinsing with TBS-T, the membranes were incubated with the HRP goat anti-rabbit IgG secondary antibody (Beijing Emarbio Science & Technology Co., Ltd.) at room temperature for 1 h. Protein bands were visualized using ECL luminophore (MilliporeSigma) and an enhanced chemiluminescence detection system (Bio-Rad Laboratories, Inc.). Protein expression was semi-quantified using ImageJ software v1.53e (National Institutes of Health). For the MAPK pathway detection, vinculin (124 kDa) was used as internal reference as it has been widely used in other studies (52,53), to ensure there is no overlap with the molecular weight of the experimental proteins (40-54 kDa). In all other cases, β-actin (42 kDa) was used as the internal reference.

Alizarin red staining. Cells were fixed with 4% paraformaldehyde for 15 min at room temperature and incubated with alizarin red solution (Wuhan Servicebio Technology Co., Ltd.) at room temperature for 10 min. Cells were incubated in PBS to remove excess stain. Matrix calcium depositions were imaged using a light microscope (Zeiss AG) and subsequently dissolved in 10% cetylpyridinium chloride (Sigma-Aldrich; Merck KGaA) at room temperature for 1 h. The absorbance was measured at 562 nm using Gene5 CHS 3.11 software (BioTek; Agilent Technologies, Inc.) on a microplate reader (BioTek; Agilent Technologies, Inc.).

ELISA. Cell culture supernatants were collected from each group and centrifuged at 500 x g for 5 min at 4˚C. ELISA kits (Beijing winter song Boye Biotechnology Co. Ltd.) were used to measure the secreted cytokine expression of RANKL (Mouse RANKL ELISA Kit; cat. no. DG30574M), osteoprotegerin (OPG; Mouse OPG ELISA Kit; cat. no. DG30295M), IL-6 (Mouse IL-6 ELISA Kit; cat. no. DG30754M), TNF-α (Mouse TNF-α ELISA Kit; cat. no. DG30048M) and IL-1β (Mouse IL-1β ELISA Kit; cat. no. DG94767Q) according to the manufacturer's protocol.

RNA stability. Cells were treated with 5 μg/ml actinomycin D (ACMEC biochemical) at 37˚C to inhibit mRNA transcription. Total RNA was extracted at 0, 3 and 6 h. RT-qPCR was carried out as aforementioned to examine mRNA expression and calculate the degradation rate of target genes, which was presented as the relative expression of mRNA at each time point relative to that at the 0-h timepoint (54).

Cell transfection. Specific lentiviral vectors carrying short hairpin RNA (shRNA/sh) or control shRNA (GeneChem, Inc.) were used for Mettl3 knockdown. shRNA sequences are shown in Table SIII. Lentiviral vectors were used for Mettl3 overexpression, and blank vectors were prepared by Guangzhou IGE Biotechnology, Ltd. shRNA sequences were synthesized and Mettl3 overexpression products were amplified. The lentivirus transfer plasmid pLVX (Thermo Fisher Scientific, Inc.)-shRNA was used for recombinant plasmid construction and lentivirus production. And for Mettl3 overexpression, pCDH-CMV-MCS-EF1-copGFP-T2A-Puro vector (Thermo Fisher Scientific, Inc.) was employed and the Mettl3 coding region was inserted into the MCS sites of the vector. At 18 h before transfection, HEK 293T cells (Procell Life Science &Technology Co., Ltd.) were inoculated in six-well cell culture plates at a density of $4x10^5$ cells per well. Before transfection, 2 μg of the plasmid was diluted in 100 μl Opti-MEM medium (Gibco) without serum (tube A), and 6 μl polyethylenimine reagent was diluted in another 100 μl serum-free Opti-MEM (tube B). We then added the dilution in tube B into tube A and mixed it gently. The mixture was incubated at room temperature for 12 min and then added to the cell culture medium. A 3rd generation system including four-plasmid lentivirus, pLP/VSVG, pLP1, pLP2, and empty/recombinant pLVX vector (Thermo Fisher Scientific, Inc.), was applied at a molar ratio of 1:1:1:2. Cells were incubated with transfection reagent-plasmid mixture at 37˚C for 6 h before replacement. At 24 h after replacement, cell culture medium containing lentiviral particles was collected. The above protocols were completed by company and we carried out the subsequent transfection and selection. In brief, lentiviruses were cultured with MC3T3-E1 cells at a MOI of 50 at 37˚C for 12 h. Green fluorescence protein labeling was used to observe transfection using a light microscope (Zeiss AG). Cell lines with stable expression were selected using 6 μg/ml puromycin for 3 days and maintained using 2 μg/ml puromycin (Biosharp Life Sciences). For YTH domain family 2 (Ythdf2) knockdown, 50 nM small interfering RNA (si)Ythdf2 or NC (Guangzhou IGE Biotechnology, Ltd.), named siCtrl, was employed to transfect cells with the addition of Lipofectamine® 2000 Transfection reagent (Biosharp Life Sciences) at 37˚C for 24 h (Table SIII). The transfected cells were employed for subsequent experimentations at 24 h after transfection. The transfection efficiency was determined using RT-qPCR and western blot analysis and at 24 and 48 h after the transfection, respectively.

RNA dot blot for total m^6A content analysis. Total RNA was extracted as aforementioned and incubated at 95˚C for 3 min to disrupt secondary structures. Denatured total RNA was loaded onto nitrocellulose membranes and subsequently crosslinked to the membrane with UV light at 254 nm for 30 min. Unbound RNA was removed by washing with TBS-T. Western blot analysis was carried out as aforementioned using the anti-m^6A antibody (Table SII).

Methylated RNA immunoprecipitation (MeRIP)-qPCR. The EpiQuik CUT&RUN m^{6}A RNA Enrichment kit (EpigenTek Group, Inc.) was used for the MeRIP assay as previously described (55,56). Briefly, total RNA was collected and randomly fragmented. RNA fragments were immunoprecipitated with magnetic beads pre-coated with anti-immunoglobulin (IgG), anti-m^{6}A or anti-Ythdf2 antibodies. Targeted RNA fragments were released, purified and eluted, followed by RT-qPCR as aforementioned. Relative enrichment was normalized to the input sample.

Statistical analysis. All data were representative of three independent experiments and presented as the mean ± standard deviation. Data were plotted and analyzed using GraphPad Prism v9.0 (Dotmatics). Comparisons between two groups were analyzed using an unpaired Student's t-test. Comparisons among multiple groups were analyzed using one-way ANOVA followed by Tukey's post hoc test and two-way ANOVA followed by Bonferroni's post hoc test. $P<0.05$ was considered to indicate a statistically significant difference.

Results

Titanium particles inhibit osteogenic differentiation and mediate osteoblast-osteoclast communication. Titanium particles engulfed into osteoblastic cells were observed using TEM (Fig. 1A). In the present study, RT-qPCR and western blot analysis were used to show early trends, and alizarin red staining was used to study later trends. The results of the present study demonstrated that titanium particle treatment significantly inhibited the expression of osteogenesis-associated markers and the formation of calcium nodules compared with those in the osteogenic induction group (Fig. 1B and C). Furthermore, titanium particles induced the mRNA expression of proinflammatory cytokines (Fig. 1D), and these results were verified via ELISA. To further investigate the regulatory role of titanium particles in osteoblast-osteoclast communication, which is critical for bone homeostasis (57), the supernatant of titanium-treated osteoblasts was harvested and co-cultured with preosteoclasts. As shown in Fig. 1E, mRNA and protein expression levels of markers associated with osteoclast differentiation of RAW264.7 cells were increased in the titanium particle treatment group (CM) compared with the NC group. Thus, the expression levels of additional soluble factors released from osteoblasts that mediate osteoblast-osteoclast communication were investigated. Notably, RANKL expression was significantly increased, leading to a higher ratio of RANKL/OPG (Fig. 1F).

Role of m^{6}A modification in titanium particle treatment. To explore the role of m^{6}A modification in titanium particle treatment of osteoblasts, m^{6}A levels were evaluated. The results of the RNA dot blot analysis demonstrated that m^{6}A levels were reduced in the titanium treatment group compared with the osteogenic induction group (Fig. 2A). Subsequently, expression levels of common methyltransferases and demethylases were further determined via RT-qPCR and western blotting (Fig. 2B and C). The expression levels of Mettl3, a key methyltransferase, were significantly decreased during titanium treatment, and these results were consistent with the measurement of m^{6}A levels.

Mettl3 knockdown induces osteogenic inhibition and proinflammatory responses. To explore the association between titanium particle-induced bioactivities and the reduced expression levels of Mettl3, Mettl3 knockdown was carried out in MC3T3-E1 cells, referred to as shMettl3 cells (Fig. 3A). The results of the present study demonstrated that Mettl3 mRNA and protein expression was significantly reduced following transfection compared with the NC or blank groups (Fig. 3B). The results of the RNA dot blot analysis revealed that m^{6}A levels were lowest in the shMettl3 group compared with the control and titanium particle treatment groups (Fig. 3C). Notably, mRNA and protein expression levels of osteogenic markers were significantly reduced in the shMettl3 group (Fig. 3D). In addition, the alizarin red staining assay demonstrated consistent results, indicating that Mettl3 knockdown induced osteogenic inhibition comparable with that induced by titanium particles (Fig. 3D). Furthermore, Mettl3 knockdown increased the expression of proinflammatory cytokines (Fig. 3E). Mettl3 knockdown increased the RANKL expression and the ratio of RANKL/OPG compared with the control group (shCtrl osteoblasts without titanium particle) (Fig. 3F). Additionally, the supernatant of Mettl3-knockdown osteoblasts was harvested and co-cultured with RAW264.7 cells. mRNA and protein expression levels of markers associated with osteoclastogenesis were increased in RAW264.7 cells cultured with supernatant of Mettl3-knockdown osteoblasts compared with the control group (shCtrl osteoblasts without titanium particle) (Fig. 3G).

Mettl3 overexpression attenuates titanium particle-induced inhibition of osteogenesis and proinflammatory activities. To further verify whether titanium particles mediated the aforementioned activities through reduced Mettl3 expression, a Mettl3-overexpression osteoblast cell line was constructed, and a blank vector was used as the NC. RT-qPCR and western blotting were performed to determine the transfection efficiency following overexpression (Fig. 4A). TEM analysis demonstrated that Mettl3 overexpression did not impact the engulfment capability of osteoblasts (Fig. 4B). Notably, m^{6}A levels in the Mettl3 overexpression group were significantly increased compared with those in the blank group (Fig. 4C). The results of the present study also demonstrated that Mettl3 overexpression attenuated titanium-induced inhibition of osteogenesis (Fig. 4D). In addition, titanium-induced proinflammatory activities were also attenuated, as well as the ratio of RANKL/OPG (Fig. 4E and F). The aforementioned results in Fig. 1E indicated the regulatory role of titanium particles in osteoblast-osteoclast communication, while this indirect regulatory effect of titanium particles on osteoclastogenesis of RAW264.7 cells was also reversed by Mettl3 overexpression (Fig. 4G).

Titanium particle treatment targets Smad7 and SMAD specific E3 ubiquitin protein ligase 1 (Smurf1) via Mettl3, leading to bone morphogenetic protein (BMP) signaling inhibition. To explore the downstream signaling molecules affected by Mettl3, the canonical BMP-Smad signaling pathway was evaluated. The

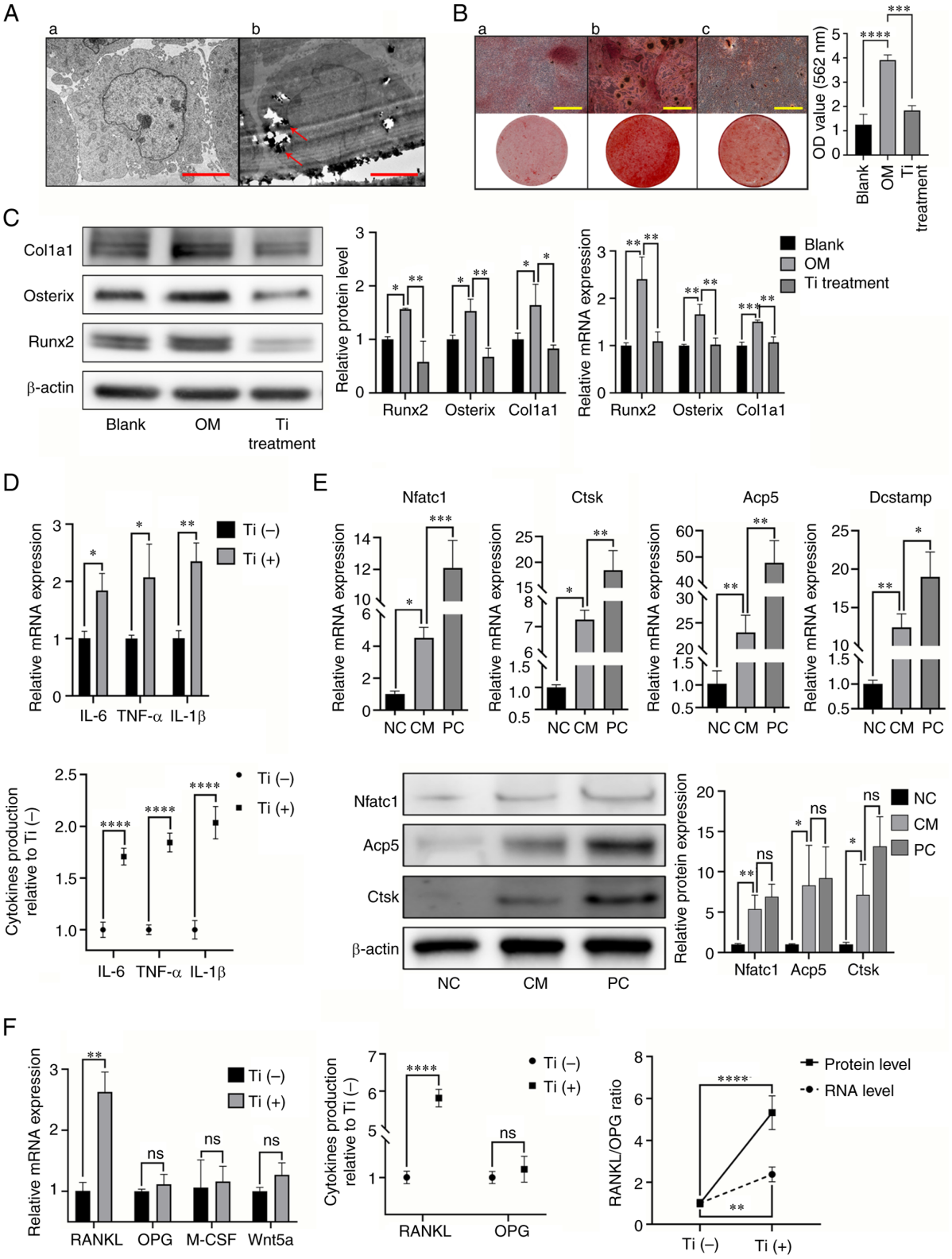

Figure 1. Titanium particles inhibit osteogenic differentiation and mediate osteoblast-osteoclast communication. (A) Transmission electron microscopy of osteoblasts co-cultured (A-a) without and (A-b) with titanium particles (red arrows; scale bar, 5 μm). (B) Titanium particle treatment inhibited the formation of mineralized nodules at 14 days. (B-a) Blank, (B-b) osteogenic induction medium and (B-c) titanium particle treatment. Scale bar, 500 μm. (C) Titanium particle treatment inhibited the expression of osteogenesis-associated markers. The samples were collected at 2 and 3 days for RT-qPCR and western blotting, respectively. (D) Titanium particle treatment promoted the expression of inflammatory cytokines. The samples were collected at 2 and 3 days for RT-qPCR and ELISA, respectively. (E) Supernatants of titanium-treated osteoblasts promoted the expression of osteoclast differentiation-associated markers in preosteoclasts. (F) Titanium treatment promoted the expression of RANKL, leading to the higher ratio of RANKL/OPG. The samples were collected at 2 and 3 days for RT-qPCR and ELISA, respectively. Data are representative of three independent experiments and are presented as the mean ± standard deviation. *P<0.05, **P<0.01, ***P<0.001 and ****P<0.0001. Acp5, acid phosphatase 5, tartrate resistant; Col1a1, collagen type I α1 chain; Ctsk, cathepsin K; CM, conditioned medium; Dcstamp, dendrocyte expressed seven transmembrane protein; M-CSF, macrophage colony-stimulating factor; NC, negative control; Nfatc1, nuclear factor of activated T cells 1; ns, not significant; OD, optical density; OM, osteogenic induction medium; OPG, osteoprotegerin; PC, positive control; RANKL, receptor activator of NF-κB ligand; RT-qPCR, reverse transcription-quantitative PCR; Runx2, RUNX family transcription factor 2; Ti, titanium particle.

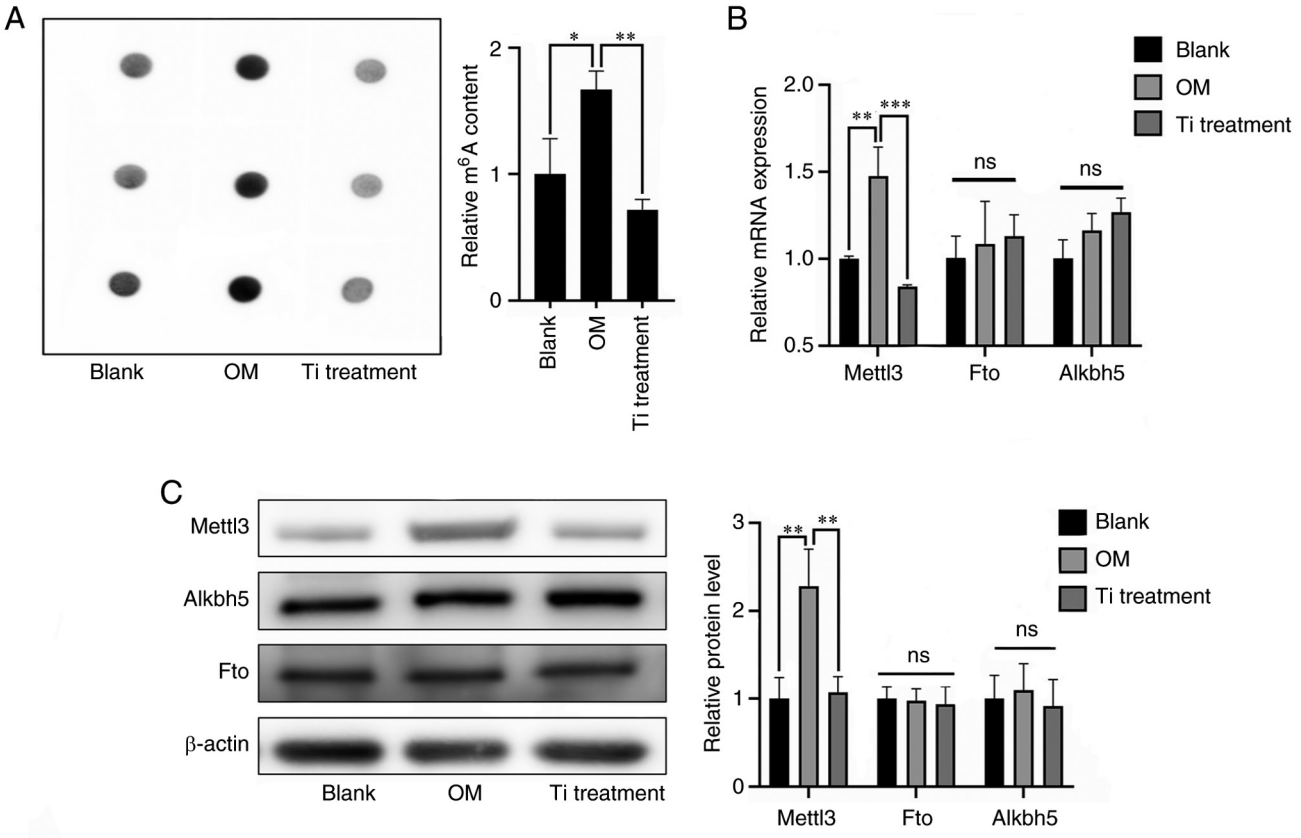

Figure 2. Role of m^{6}A modification in titanium particle treatment. (A) Titanium particle treatment reduced total m^{6}A levels compared with the osteogenic induction group after 2 days. (B) Titanium particle treatment significantly reduced the mRNA expression of the methylation-associated enzyme Mettl3. Samples were collected at 2 days for reverse transcription-quantitative PCR. (C) Titanium particle treatment significantly reduced the protein expression levels of Mettl3. Samples were collected at 3 days for western blotting. Data are representative of three independent experiments and are presented as the mean ± standard deviation. *P<0.05, **P<0.01 and ***P<0.001. Alkbh5, alkB homolog 5, RNA demethylase; Fto, FTO α-ketoglutarate dependent dioxygenase; m^{6}A, N6-methyladenosine; Mettl3, methyltransferase-like 3; ns, not significant; OM, osteogenic induction medium; Ti, titanium particle.

results of RT-qPCR analysis demonstrated that titanium particle treatment increased Smad7 and Smurf1 expression in osteoblasts, while Mettl3 overexpression attenuated the upregulated expression of Smad7 and Smurf1 induced by titanium particle treatment (Fig. 5A). The results of western blotting further demonstrated that titanium particle treatment inhibited the phosphorylation levels of Smad1/5/9 and induced the increased expression of Smad7 and Smurf1, and these reactions induced by titanium particle treatment were also reversed by Mettl3 overexpression (Fig. 5B). The results of the present study also demonstrated that both titanium particle treatment and Mettl3 knockdown increased the mRNA stability of these two genes, leading to increased expression levels (Fig. 5C). Furthermore, MeRIP-qPCR analysis revealed that the m^{6}A enrichment of Smad7 and Smurf1 transcripts was significantly reduced in the titanium particle treatment and Mettl3 knockdown groups compared with the control group (Fig. 5D).

Titanium particles induce NOD-like receptors (NLRs) to exert proinflammatory activities. The results of western blotting revealed that titanium particle treatment induced the activation of the MAPK and NF-κB pathways, while Mettl3 overexpression attenuated this activation. For p38, it seemed that the titanium particle induced its activation while the Mettl3 overexpression failed to attenuated this activation. (Fig. 6A). The expression changes of key components of the NLR signaling pathway were also evaluated. The results of the present study demonstrated that titanium particle treatment increased the expression and the mRNA half-life of NOD1 and receptor interacting serine/threonine kinase 2 (RIPK2) in osteoblasts. However, the mRNA stability and expression of NOD2 were not enhanced (Fig. 6B and C). MeRIP-qPCR analysis demonstrated that NOD1 and RIPK2 transcripts functioned as the target of Mettl3, as titanium particle treatment and Mettl3 knockdown both significantly reduced the m^{6}A enrichment of these two transcripts compared with the control group (Fig. 6D).

To further verify the role of the NLR1 signaling pathway in the titanium particle-induced inflammatory response, cells were pretreated with ML130 (NOD1 inhibitor) and WEHI-345 (RIPK2 inhibitor) to block the NOD1 pathway since titanium particles can act on both NOD1 and RIPK2 mRNA based on the aforementioned results. In Fig. 7A, without the addition of inhibitors, titanium particle induced the activation of the MAPK and NF-κB signaling pathways, and the activation of these two pathways was significantly inhibited following treatment with both inhibitors from the comparison between titanium particle treatment without inhibitors group and titanium particle treatment with inhibitors group (Fig. 7A). In addition, inhibition of the NOD1 pathway attenuated the titanium particle-induced increased expression of IL-6, TNF-α, IL-1β

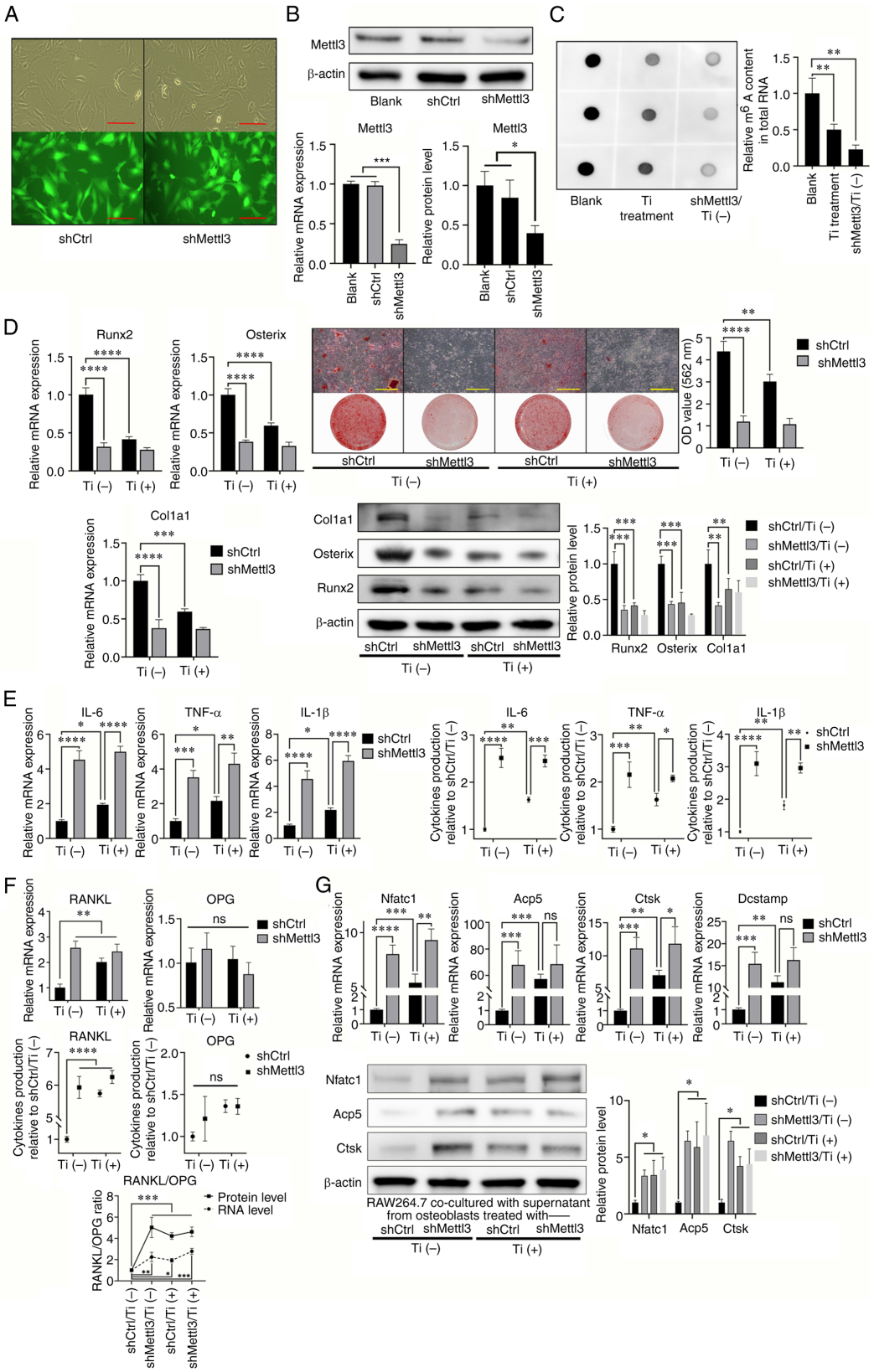

Figure 3. Mettl3 knockdown induces osteogenic inhibition and proinflammatory responses. (A) Construction of Mettl3 knockdown cells (scale bar, 100 μm). (B) The verification of transfection efficiency using reverse transcription-quantitative PCR and western blotting. (C) Mettl3 knockdown and titanium particle treatment were associated with reduced m^{6}A content in total RNA compared with the blank group (osteoblasts without transfection). (D) Mettl3 knockdown inhibited the expression of osteogenic markers and the formation of mineralized nodules (scale bar, 500 μm). (E) Mettl3 knockdown promoted the expression of inflammatory cytokines. (F) Mettl3 knockdown led to a higher ratio of RANKL/OPG compared with that of the control group (shCtrl cells without Ti). (G) Supernatant of Mettl3 knockdown osteoblasts promoted the expression of osteoclast differentiation-associated markers in preosteoclasts. Data are representative of three independent experiments and are presented as the mean ± standard deviation. *P<0.05, **P<0.01, ***P<0.001 and ****P<0.0001. Acp5, acid phosphatase 5, tartrate resistant; Col1a1, collagen type I α1 chain; Ctrl, control; Ctsk, cathepsin K; Dcstamp, dendrocyte expressed seven transmembrane protein; m^{6}A, N6-methyladenosine; Mettl3, methyltransferase-like 3; Nfatc1, nuclear factor of activated T cells 1; ns, not significant; OD, optical density; OPG, osteoprotegerin; RANKL, receptor activator of NF-κB ligand; sh, short hairpin RNA; Runx2, RUNX family transcription factor 2; Ti, titanium particle.

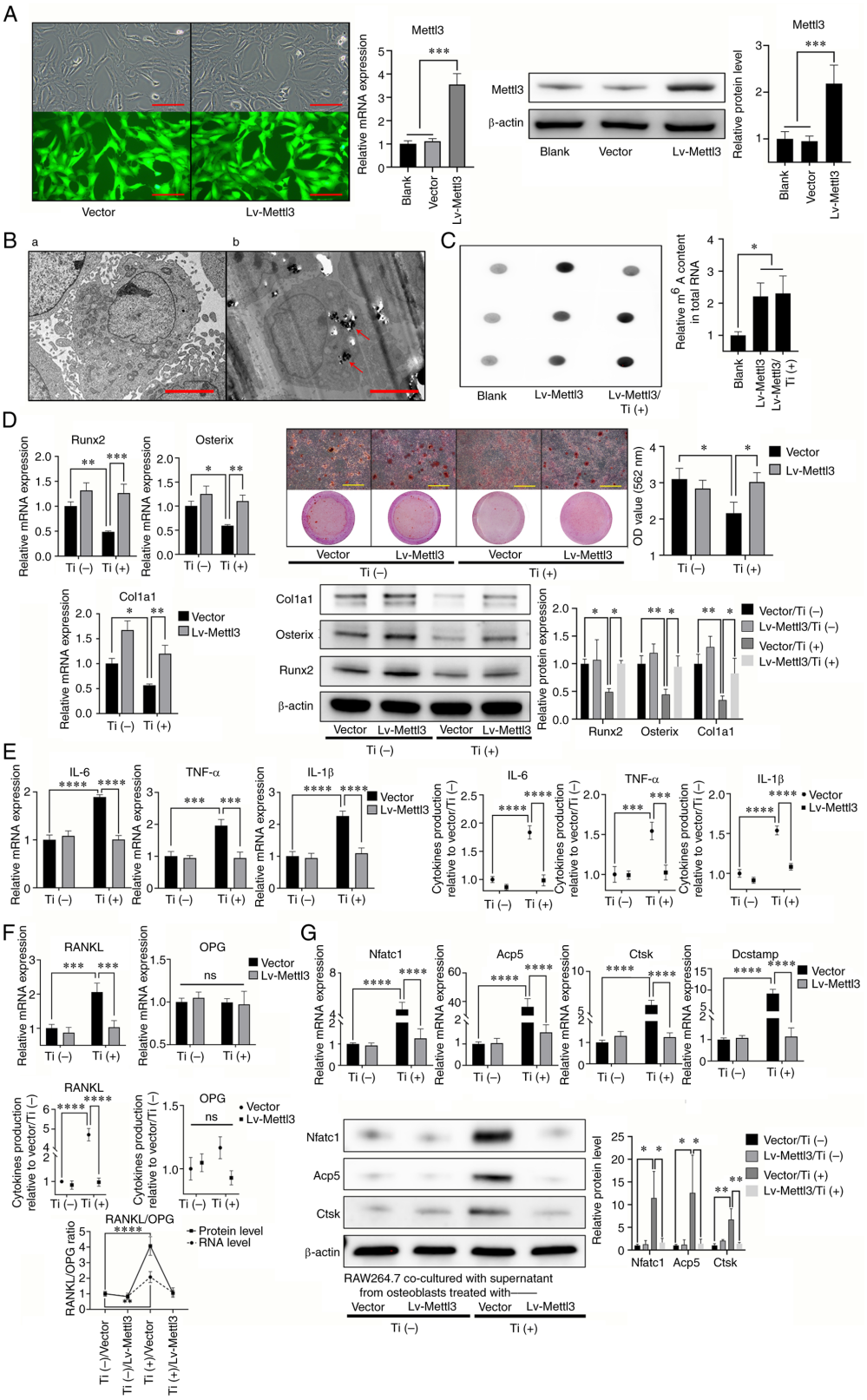

Figure 4. Mettl3 overexpression attenuates titanium particle-induced osteogenesis inhibition and proinflammatory responses. (A) Construction of Mettl3 overexpression cells and the verification of transfection efficiency using reverse transcription-quantitative PCR and western blotting (scale bar, 100 μm). (B) Transmission electron microscopy of Mettl3 overexpression cells co-cultured (B-a) without or (B-b) with titanium particles (red arrows; scale bar, 5 μm). (C) Mettl3 overexpression increased the m^{6}A content in total RNA compared with that of the blank group (osteoblasts without transfection). (D) Mettl3 overexpression attenuated titanium particle-induced osteogenesis inhibition (scale bar, 500 μm). (E) Mettl3 overexpression attenuated titanium particle-induced proinflammatory responses. (F) Mettl3 overexpression attenuated the titanium particle-induced increase in the RANKL/OPG ratio. (G) Mettl3 overexpression attenuated osteoclast differentiation promotion induced by the supernatant of Ti-treated osteoblasts. Data are representative of three independent experiments and are presented as the mean ± standard deviation. *P<0.05, **P<0.01, ***P<0.001 and ****P<0.0001. Acp5, acid phosphatase 5, tartrate resistant; Col1a1, collagen type I α1 chain; Ctsk, cathepsin K; Dcstamp, dendrocyte expressed seven transmembrane protein; Lv, lentivirus; m^{6}A, N6-methyladenosine; Mettl3, methyltransferase-like 3; Nfatc1, nuclear factor of activated T cells 1; ns, not significant; OD, optical density; OPG, osteoprotegerin; RANKL, receptor activator of NF-kB ligand; Runx2, RUNX family transcription factor 2; Ti, titanium particle.

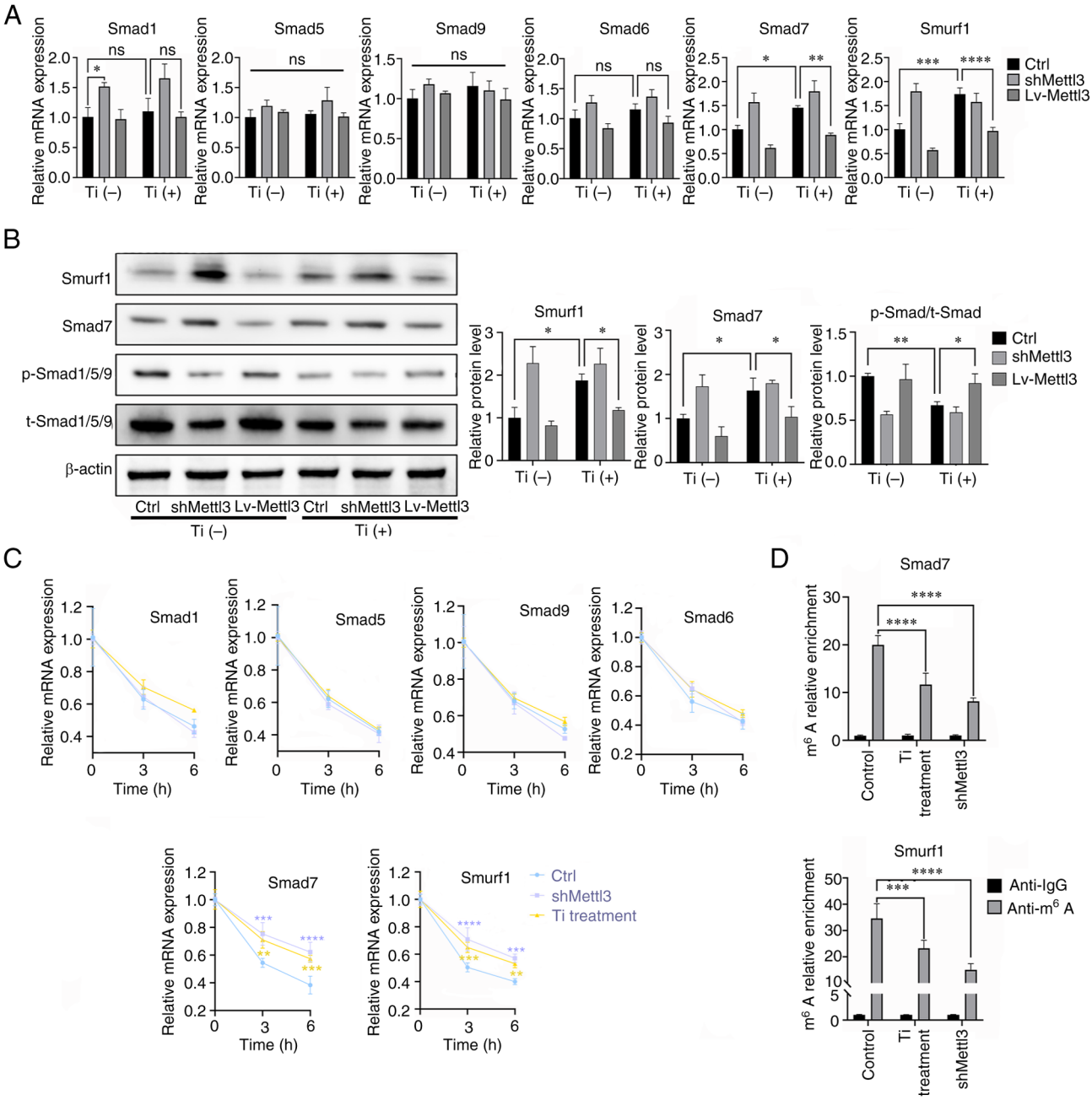

Figure 5. Titanium particle treatment targets Smad7 and Smurf1 via Mettl3, leading to BMP signaling inhibition. (A) Effects of titanium particle treatment and Mettl3 knockdown/overexpression on the mRNA expression of key signaling molecules of BMP signaling. (B) Effects of titanium particle treatment and Mettl3 knockdown/overexpression on BMP signaling activation. (C) Titanium particle treatment enhanced the mRNA stability of Smad7 and Smurf1 transcripts at the selected timepoints, following the addition of actinomycin D. (D) Titanium particle treatment significantly decreased the m^{6}A modification of these two transcripts. The control group in this figure were osteoblasts without transfection. Data are representative of three independent experiments and are presented as the mean ± standard deviation. *P<0.05, **P<0.01, ***P<0.001 and ****P<0.0001. BMP, bone morphogenetic protein; Ctrl, control; Lv, lentivirus; m^{6}A, N6-methyladenosine; Mettl3, methyltransferase-like 3; ns, not significant; p-, phosphorylated; sh, short hairpin RNA; Smurf1, SMAD specific E3 ubiquitin protein ligase 1; t-, total; Ti, titanium particle.

and RANKL (Fig. 7B). Collectively, these data suggested that titanium particles may target the NOD1 signaling pathway to regulate subsequent inflammatory responses.

Ythdf2 participates in the Mettl3-mediated osteogenic inhibition and proinflammatory activities in titanium particle treatment. m^{6}A readers recognize m^{6}A modifications and then mediate regulatory effects, including RNA translation, decay and splicing (41). The aforementioned results (Figs. 5D and 6D) revealed that downregulated Mettl3 levels led to the enhancement of mRNA stabilities of Smad7, Smurf1, NOD1 and RIPK2, and thus, it was hypothesized that it was Ythdf2 that exerted the effects. Firstly, siYthdf2 was used to knockdown its expression (Fig. 8A). The mRNA and protein expression levels of Smad7, Smurf1, NOD1 and RIPK2 were increased in the Ythdf2 knockdown group compared with the control group (Fig. 8B). The mRNA stabilities of these four mRNAs were also enhanced in Ythdf2 knockdown cells at 3 and 6 h, while

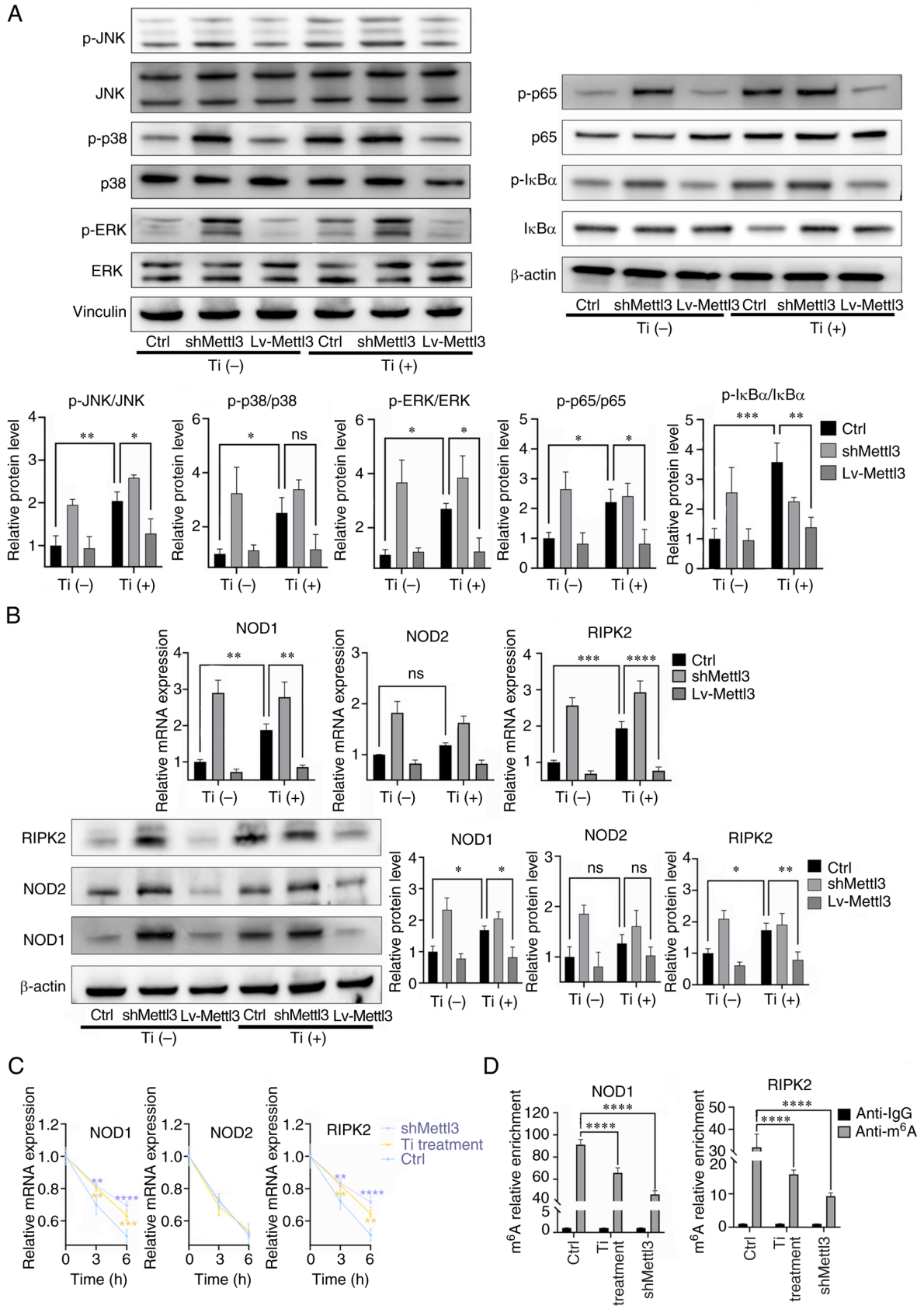

Figure 6. Titanium particle treatment induces NOD-like receptors to exert proinflammatory responses. (A) Titanium particle treatment induced the activation of the MAPK and NF-κB signaling pathways. (B) Titanium particle treatment induced the activation of the NOD-like receptor pathway, while Mettl3 overexpression attenuated these effects. (C) Titanium particle treatment and Mettl3 knockdown enhanced the mRNA stabilities of NOD1 and RIPK2 following the addition of actinomycin D. (D) Titanium particle treatment and Mettl3 knockdown decreased the m^{6}A modification of NOD1 and RIPK2. The control group in this figure were osteoblasts without transfection. Data are representative of three independent experiments and are presented as the mean ± standard deviation. *P<0.05, **P<0.01, ***P<0.001 and ****P<0.0001. Ctrl, control; Lv, lentivirus; m^{6}A, N6-methyladenosine; Mettl3, methyltransferase-like 3; NOD, nucleotide binding oligomerization domain; ns, not significant; p-, phosphorylated; RIPK2, receptor interacting serine/threonine kinase 2; sh, short hairpin RNA; Ti, titanium particle.

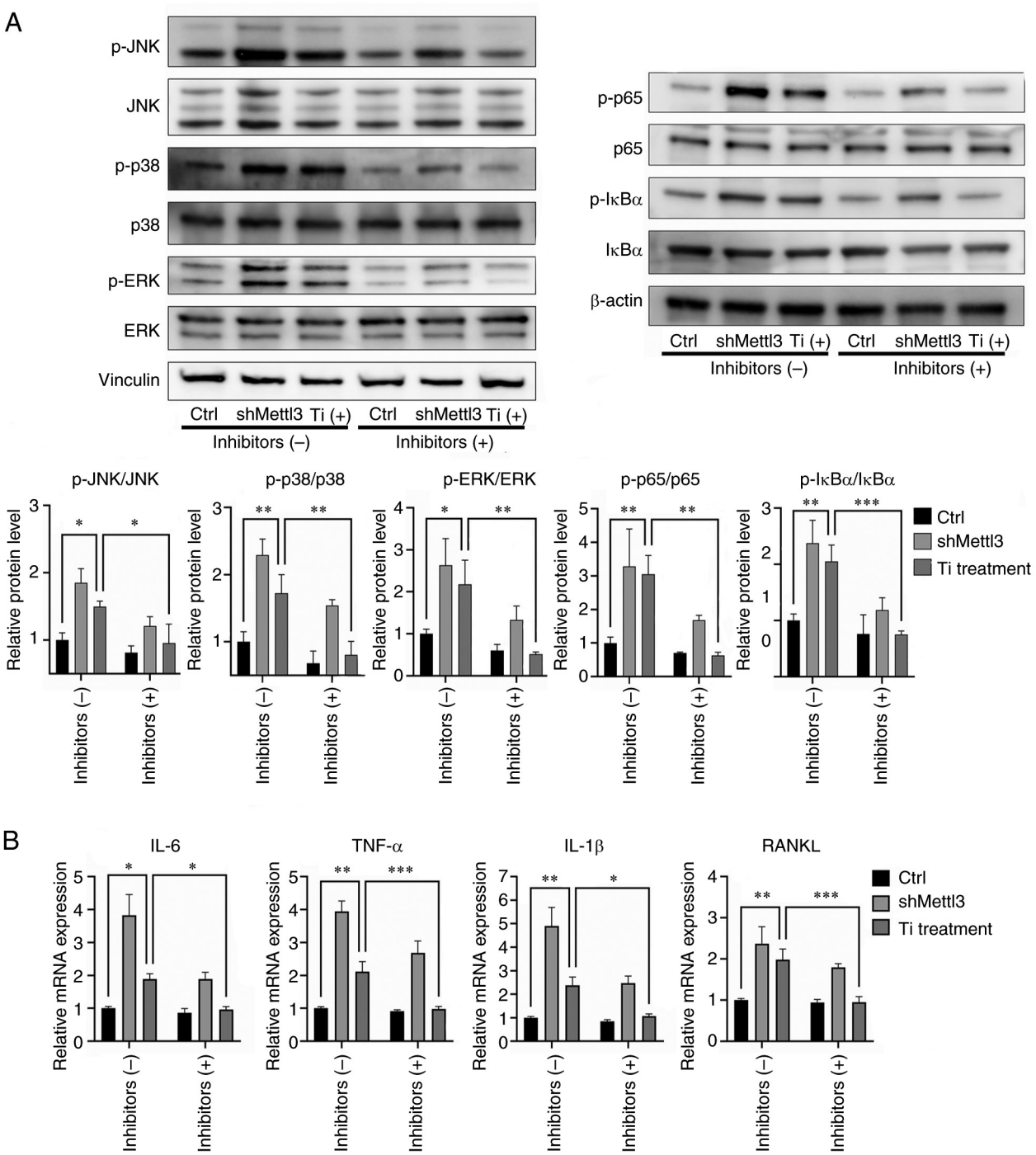

Figure 7. Inhibition of the NOD-like receptor signaling pathway inhibits titanium particle-induced proinflammatory responses. (A) Inhibition of the NOD1 signaling pathway inhibited MAPK and NF-κB signaling activation induced by titanium particle treatment. (B) Inhibition of the NOD1 signaling pathway inhibited proinflammatory cytokine expression induced by titanium particle treatment. The control group in this figure were osteoblasts without inhibitors. Data are representative of three independent experiments and are presented as the mean ± standard deviation. *P<0.05, **P<0.01 and ***P<0.001. Ctrl, control; Mettl3, methyltransferase-like 3; NOD, nucleotide binding oligomerization domain; p-, phosphorylated; sh, short hairpin RNA; Ti, titanium particle.

the stability of NOD at 6 h didn't show statistical difference (Fig. 8C), suggesting that Ythdf2 could affect the expression of these four mRNAs by regulating their stabilities. In Fig. 8D, we measured the relative expressions of these four mRNAs precipitated by Ythdf2, which were shown in anti-Ythdf2 column. Notably, titanium particle treatment reduced the expression levels of these mRNAs compared with control group, indicating that the binding between Ythdf2 and mRNAs was significantly decreased following titanium particle treatment (Fig. 8D).

Discussion

Bone homeostasis is a dynamic balance regulated by osteoblasts and osteoclasts. However, dysregulation of the balance between osteoblasts and osteoclasts may result in pathological bone loss, in which osteogenic inhibition and inflammatory responses serve a vital role (57,58). The activation of inflammatory responses promotes the secretion of several cytokines and the regulation of specific cell types, including osteoclasts,

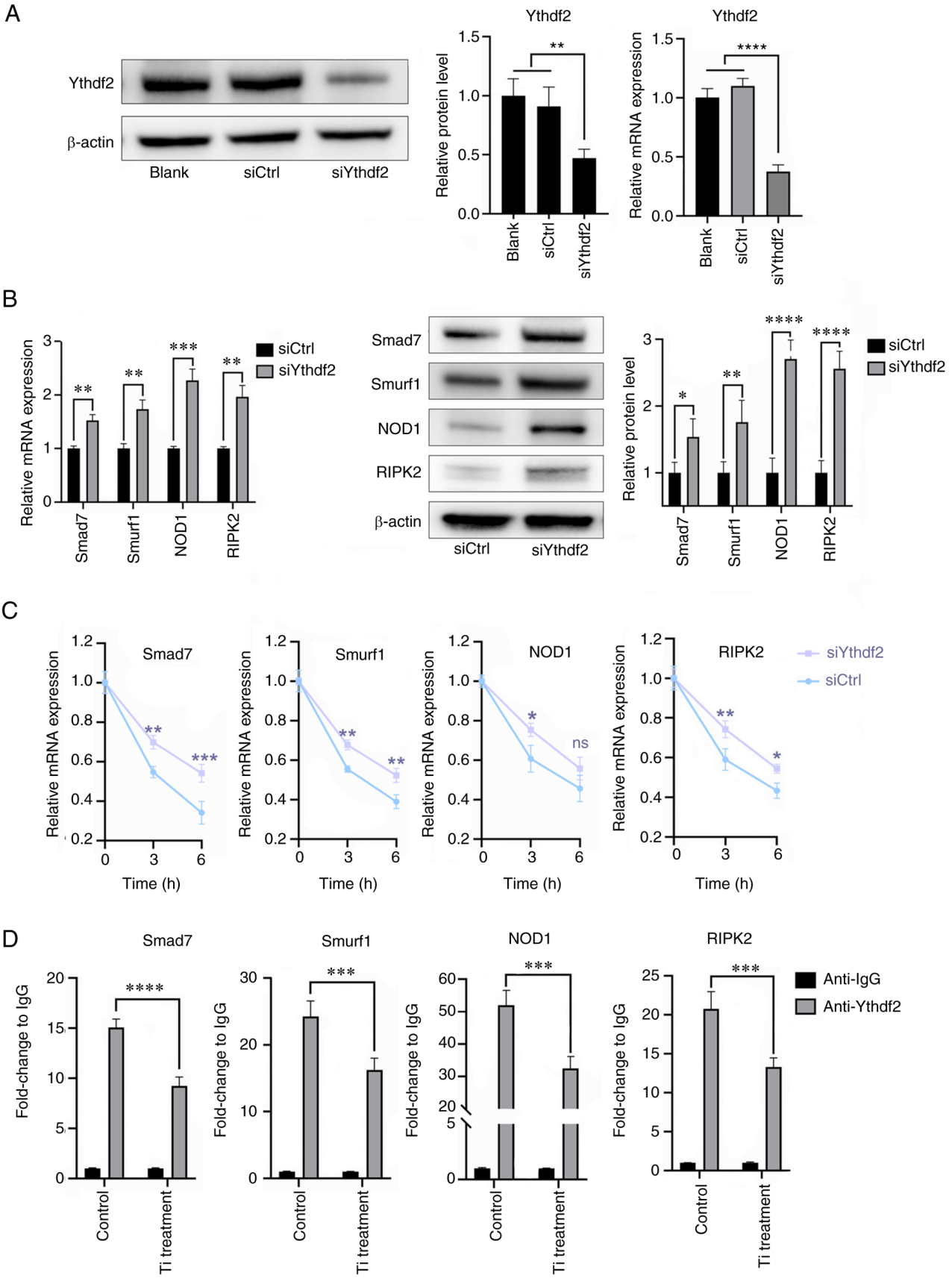

Figure 8. Ythdf2 participates in the methyltransferase-like 3-mediated bioactivities in titanium particle treatment. (A) Knockdown of Ythdf2 and verification of transfection efficiency using reverse transcription-quantitative PCR and western blotting. (B) Ythdf2 knockdown promoted the expression of Smad7, Smurf1, NOD1 and RIPK2. (C) Ythdf2 knockdown enhanced the mRNA stabilities of Smad7, Smurf1, NOD1 and RIPK2 at 3 h. (D) Methylated RNA immunoprecipitation-quantitative PCR results demonstrated that titanium particle treatment decreased the relative expression levels of Smad7, Smurf1, NOD1 and RIPK2 precipitated by Ythdf2. Data are representative of three independent experiments and are presented as the mean ± standard deviation. *P<0.05, **P<0.01, ***P<0.001 and ****P<0.0001. Ctrl, control; NOD, nucleotide binding oligomerization domain; RIPK2, receptor interacting serine/threonine kinase 2; si, small interfering RNA; Smurf1, SMAD specific E3 ubiquitin protein ligase 1; Ythdf2, YTH domain family 2; Ti, titanium particle.

osteoblasts, macrophages and immune cells, thus leading to pathological osteolysis (57,59). The results of the present study revealed that titanium particles inhibited osteogenesis and proinflammatory responses, and these results are consistent with previous reports (10,22,60). Furthermore, the results of the present study demonstrated that titanium particles mediated the osteoblast-osteoclast communication, leading to enhanced osteoclast activity, and these underlying mechanisms were primarily explored. Notably, osteoblasts secrete several soluble factors, including macrophage colony-stimulating factor, RANKL, OPG and WNT5A, to act on osteoclasts (57). The elevated RANKL/OPG ratio may contribute to the enhanced osteoclast activity. However, additional mechanisms, such as secreted exosomes and membrane-bound mediators, were not further explored in the present study.

Previous studies have reported the critical role of m^6A methylation in bone remodeling and inflammation (48,61). To explore the potential role of m^6A methylation in titanium particle-induced bioactivities, total m^6A levels were determined. Notably, the differentially expressed enzyme Mettl3 is the most critical methyltransferase and previous studies have indicated that Mettl3 exerts regulatory effects in several physiological and pathological processes (42-47). The results of the present study demonstrated that Mettl3 knockdown induced the inhibition of osteogenesis and proinflammatory responses, and these effects were comparable to those induced by titanium particles. In addition, Mettl3 overexpression reversed the bioactivities induced by titanium particles. Previous studies have demonstrated that Mettl3-mediated m^6A modification regulated bone metabolism, including cell differentiation, and abnormal Mettl3 expression levels may induce bone metabolic diseases (44,46,48). Collectively, the results of the present study highlighted that Mettl3 may function as an upstream regulator in titanium particle-induced bioactivities.

Notably, the canonical Smad-dependent pathway serves a key role in osteogenesis and the activation and translocation of the Smad1/5/9 complex triggers the subsequent expression of osteogenesis-related genes (62,63). Inhibitory Smads negatively regulate Smad signaling by preventing Smad1/5/9 activation and degrading Smad1/5/9 with the assistance of the E3 ubiquitin ligase, Smurf1 (62,64). Thus, RT-qPCR and western blotting revealed the decreased levels of Smad1/5/9 phosphorylation, along with the increased expression of Smad7 and Smurf1, following treatment with titanium particles or Mettl3 knockdown. Notably, enhanced mRNA stability may account for the increased expression of Smad7 and Smurf1. To further confirm the regulation of Mettl3, MeRIP-qPCR was performed. The results of the present study indicated that the m^6A enrichment of these two transcripts was significantly reduced following titanium particle treatment or Mettl3 knockdown. Thus, titanium particle treatment may suppress the mRNA decay of Smad7 and Smurf1 via Mettl3 downregulation, leading to inhibition of Smad-dependent signaling.

Previous studies have demonstrated that titanium particles may concurrently activate two classical proinflammatory pathways, including the MAPK and NF-κB pathways, and promote the expression of downstream proinflammatory cytokines (26,27,65). The results of the present study demonstrated that titanium particle treatment induced the activation of these two inflammation-associated pathways, while Mettl3 overexpression reversed the activation, suggesting that Mettl3 was involved in the activation of the MAPK and NF-κB signaling pathways. To further explore the target of titanium particles in these pathways, the mRNA stability of numerous molecules was determined. A previous study identified the activation of the NLR signaling pathway in Mettl3 knockdown macrophages via RNA sequencing analysis (66). Activation of key members of the NLR pathway, including NOD1, NOD2 and RIPK2, may trigger the subsequent activation of the MAPK and NF-κB signaling pathways (67-69). Thus, it was hypothesized that titanium particles may impact the NLR pathway, leading to the subsequent activation of inflammatory responses. Notably, titanium particle treatment increased the mRNA expression and stability of NOD1 and RIPK2. In addition, the m^6A enrichment of these two transcripts was significantly reduced following titanium particle treatment. Inhibition of the NLR pathway inhibited the activation of MAPK and NF-κB pathways and the expression of proinflammatory cytokines, suggesting that titanium particles exert their effect via downregulation of Mettl3, which activates the NLR pathway and leads to the subsequent activation of inflammatory responses.

The m^6A reader proteins are required to recognize and bind to the m^6A modified transcript to regulate gene expression (70). Several m^6A readers have been identified, including YTH domain-containing family proteins, heterogeneous nuclear ribonucleoproteins, insulin like growth factor 2 mRNA binding protein families and eukaryotic initiation factor (71). Ythdf2, a main member of the YTH domain-containing family proteins, is the most extensively studied m^6A reader. Ythdf2 promotes targeted mRNA decay by recruiting the C-C motif chemokine receptor 4 negative on TATA-less deadenylase complex (72). Increasing evidence has indicated that Ythdf2 serves a critical role in pathological processes, including stress, viral infection and the inflammatory response (66,73-76). Considering that titanium particle treatment regulates RNA decay of specific mRNAs, it was hypothesized that Ythdf2may recognize the methylated modification of these mRNAs and promote the targeted mRNA decay. The results of the present study demonstrated that the knockdown of Ythdf2 led to significantly increased expression and enhanced stabilities of Smad7, Smurf1, NOD1 and RIPK2 transcripts at 3 h, and Smad7, Smurf1 and RIPK2 transcripts at 6 h. MeRIP-qPCR results (Figs. 5D and 6D) showed that titanium particle treatment could reduce the m^6A sites of these four mRNAs, meanwhile, binding sites between Ythdf2 and targeted mRNAs was significantly decreased following titanium particle treatment (Fig. 8D). Taken together, it might be concluded that the reduced m^6A sites of mRNAs led to the reduced recognition from Ythdf2, therefore reduced the mRNAs decay and increased the expression of these four molecules. Furthermore, it is possible that there are other reader proteins that participate in the titanium particle treatment. Previous studies have reported several m^6A methylation-regulated bioactivities involving more than one reader protein (77-79), including YTH N6-methyladenosine RNA binding protein F1, which promotes mRNA translation, and YTH N6-methyladenosine RNA binding protein F3, which mediates the translation or degradation of targeted RNA, which could be potential readers that also participate in

the titanium particle-induced bone loss (71). Further studies are needed to uncover the whole mechanism.

In addition, it is important to point out that the real-life concentration range of titanium particles within the body is wide (21). The *in vivo* concentration of particles is affected by various factors, including prosthesis type, implant time, sample location and detection method (80). It should be noted that the particle concentrations from different studies are difficult to be integrated as a specific range due to different measurement systems (81). Measured concentrations from several representative studies include 720-820 ppm (82), 66-1,734 μg/g tissue (83) and 103-5,759 μg/g tissue (84). It is possible to observe local high particle concentrations at specific timepoints for various reasons such as implant cracks (85). On the other hand, the cell density used in *in vitro* experiments can not simulate the real-life condition, and thus, it is difficult to directly employ the real-life concentration for *in vitro* experiments. The concentration used in the present study was drawn from previous studies (10,22,60); however, this specific concentration may not be physiologically relevant, which constitutes a potential limitation of the present study.

In conclusion, the results of the present study demonstrated that titanium particles reduced the expression of Mettl3, a key methyltransferase, and reduced the m^{6}A modification of specific mRNAs. The reduced methylation of these transcripts decreased the specific sites recognized by reader protein Ythdf2, therefore decreased the mRNA degradation mediated by Ythdf2. And that might account for the increased expression levels of Smad7, Smurf1, NOD1 and RIPK2 transcripts, leading to the inhibition of osteogenesis and proinflammatory responses. These findings highlighted that Mettl3 may act as an upstream regulatory molecule in titanium particle-induced osteolysis. Based on the critical functions of Mettl3 in various types of cancer, Mettl3 has been considered a potential target in cancer treatment (86). Therefore, future studies might focus on the feasibility of employing Mettl3 as a therapeutic target of PPO, so that multiple pathways can be regulated simultaneously and to reach the targeted effect. The *in vivo* application and ideal drug concentration are also topics for further research. Thus, the present study may provide novel insights into potential therapeutic targets for the aseptic loosening of titanium prostheses.

Acknowledgements

Not applicable.

Funding

The present study was supported by The Science and Technology Bureau of Nansha, Guangzhou (grant no. 2021ZD004).

Availability of data and materials

The datasets used and/or analyzed during the current study are available from the corresponding author on reasonable request.

Authors' contributions

XL, YY, XY and FD contributed to the study design. XL, YY, YH and XZ performed the experiments. EL and ZZ assisted in the data collection. ZZ and RX assisted in the data analysis. XL and YY wrote the manuscript and confirm the authenticity of all the raw data. All authors have read and approved the final version of the manuscript.

Ethics approval and consent to participate

Not applicable.

Patient consent for publication

Not applicable.

Competing interests

The authors declare that they have no competing interests.

References

1. Ollivere B, Wimhurst JA, Clark IM and Donell ST: Current concepts in osteolysis. J Bone Joint Surg Br 94: 10-15, 2012.
2. Hodges NA, Sussman EM and Stegemann JP: Aseptic and septic prosthetic joint loosening: Impact of biomaterial wear on immune cell function, inflammation, and infection. Biomaterials 278: 121127, 2021.
3. Tay ML, Matthews BG, Monk AP and Young SW: Disease progression, aseptic loosening and bearing dislocations are the main revision indications after lateral unicompartmental knee arthroplasty: A systematic review. J ISAKOS 7: 132-141, 2022.
4. Eger M, Sterer N, Liron T, Kohavi D and Gabet Y: Scaling of titanium implants entrains inflammation-induced osteolysis. Sci Rep7: 39612, 2017.
5. McArthur BA, Scully R, Patrick Ross F, Bostrom MPG and Falghren A: Mechanically induced periprosthetic osteolysis: A systematic review. HSS J 15: 286-296, 2019.
6. Eliaz N: Corrosion of metallic biomaterials: A review. Materials (Basel) 12: 407, 2019.
7. Prestat M and Thierry D: Corrosion of titanium under simulated inflammation conditions: Clinical context and in vitro investigations. Acta Biomater 136: 72-87, 2021.
8. Delanois RE, Mistry JB, Gwam CU, Mohamed NS, Choksi US and Mont MA: Current epidemiology of revision total knee arthroplasty in the United States. J Arthroplasty 32: 2663-2668, 2017.
9. Goodman SB: Wear particles, periprosthetic osteolysis and the immune system. Biomaterials 28: 5044-5048, 2007.
10. Zheng K, Bai J, Li N, Li M, Sun H, Zhang W, Ge G, Liang X, Tao H, Xue Y, *et al*: Protective effects of sirtuin 3 on titanium particle-induced osteogenic inhibition by regulating the NLRP3 inflammasome via the GSK-3β/β-catenin signalling pathway. Bioact Mater 6: 3343-3357, 2021.
11. Agarwal S: Osteolysis-basic science, incidence and diagnosis. Curr Orthop 18: 220-231, 2004.
12. Dattani R: Femoral osteolysis following total hip replacement. Postgrad Med J 83: 312-316, 2007.
13. Mouhyi J, Dohan Ehrenfest DM and Albrektsson T: The peri-implantitis: Implant surfaces, microstructure, and physicochemical aspects. Clin Implant Dent Relat Res 14: 170-183, 2012.
14. Derks J and Tomasi C: Peri-implant health and disease. A systematic review of current epidemiology. J Clin Periodontol 42 (Suppl 16): S158-S171, 2015.
15. Bauer TW: Particles and periimplant bone resorption. Clin Orthop Relat Res: 138-143, 2002.
16. Voggenreiter G, Leiting S, Brauer H, Leiting P, Majetschak M, Bardenheuer M and Obertacke U: Immuno-inflammatory tissue reaction to stainless-steel and titanium plates used for internal fixation of long bones. Biomaterials 24: 247-254, 2003.
17. Kotsakis GA and Olmedo DG: Peri-implantitis is not periodontitis: Scientific discoveries shed light on microbiome-biomaterial interactions that may determine disease phenotype. Periodontol 2000 86: 231-240, 2021.
18. Magone K, Luckenbill D and Goswami T: Metal ions as inflammatory initiators of osteolysis. Arch Orthop Trauma Surg 135: 683-695, 2015.

19. Man K, Jiang LH, Foster R and Yang XB: Immunological responses to total hip arthroplasty. J Funct Biomater 8: 33, 2017.
20. Guglielmotti MB, Olmedo DG and Cabrini RL: Research on implants and osseointegration. Periodontol 2000 79: 178-189, 2019.
21. Mombelli A, Hashim D and Cionca N: What is the impact of titanium particles and biocorrosion on implant survival and complications? A critical review. Clin Oral Implants Res 29 (Suppl 18): S37-S53, 2018.
22. Xiong L, Liu Y, Zhu F, Lin J, Wen D, Wang Z, Bai J, Ge G, Xu C, Gu Y, *et al*: Acetyl-11-keto-β-boswellic acid attenuates titanium particle-induced osteogenic inhibition via activation of the GSK-3β/β-catenin signaling pathway. Theranostics 9: 7140-7155, 2019.
23. Shah R, Penmetsa DSL, Thomas R and Mehta DS: Titanium corrosion: Implications for dental implants. Eur J Prosthodont Restor Dent 24: 171-180, 2016.
24. Urban RM, Jacobs JJ, Tomlinson MJ, Gavrilovic J, Black J and Peoc'h M: Dissemination of wear particles to the liver, spleen, and abdominal lymph nodes of patients with hip or knee replacement. J Bone Joint Surg Am 82: 457-476, 2000.
25. Choi MG, Koh HS, Kluess D, O'Connor D, Mathur A, Truskey GA, Rubin J, Zhou DX and Sung KL: Effects of titanium particle size on osteoblast functions in vitro and in vivo. Proc Natl Acad Sci USA 102: 4578-4583, 2005.
26. Fritz EA, Jacobs JJ, Glant TT and Roebuck KA: Chemokine IL-8 induction by particulate wear debris in osteoblasts is mediated by NF-kappaB. J Orthop Res 23: 1249-1257, 2005.
27. Chen D, Li Y, Guo F, Lu Z, Hei C, Li P and Jin Q: Protective effect of p38 MAPK inhibitor on wear debris-induced inflammatory osteolysis through downregulating RANK/RANKL in a mouse model. Genet Mol Res 14: 40-52, 2015.
28. Geng D, Wu J, Shao H, Zhu S, Wang Y, Zhang W, Ping Z, Hu X, Zhu X, Xu Y and Yang H: Pharmaceutical inhibition of glycogen synthetase kinase 3 beta suppresses wear debris-induced osteolysis. Biomaterials 69: 12-21, 2015.
29. Gu Y, Wang Z, Shi J, Wang L, Hou Z, Guo X, Tao Y, Wu X, Zhou W, Liu Y, *et al*: Titanium particle-induced osteogenic inhibition and bone destruction are mediated by the GSK-3β/β-catenin signal pathway. Cell Death Dis 8: e2878, 2017.
30. Wang L, Bai J, Wang Q, Ge G, Lin J, Xu N, Xu C, Xu Y, Wang Y and Geng D: Inhibition of protein phosphatase 2A attenuates titanium-particle induced suppression of bone formation. Int J Biol Macromol 142: 142-151, 2020.
31. Zhu Z, Xie Q, Huang Y, Zhang S and Chen Y: Aucubin suppresses titanium particles-mediated apoptosis of MC3T3-E1 cells and facilitates osteogenesis by affecting the BMP2/Smads/RunX2 signaling pathway. Mol Med Rep 18: 2561-2570, 2018.
32. Wang J, Tao Y, Ping Z, Zhang W, Hu X, Wang Y, Wang L, Shi J, Wu X, Yang H, *et al*: Icariin attenuates titanium-particle inhibition of bone formation by activating the Wnt/β-catenin signaling pathway in vivo and in vitro. Sci Rep 6: 23827, 2016.
33. Geng T, Sun S, Chen X, Wang B, Guo H, Zhang S and Jin Q: Strontium ranelate reduces the progression of titanium particle-induced osteolysis by increasing the ratio of osteoprotegerin to receptor activator of nuclear factor-κB ligand *in vivo*. Mol Med Rep 17: 3829-3836, 2018.
34. Batista PJ: The RNA modification N^6-methyladenosine and its implications in human disease. Genomics Proteomics Bioinformatics 15: 154-163, 2017.
35. Wang X, Zhao BS, Roundtree IA, Lu Z, Han D, Ma H, Weng X, Chen K, Shi H and He C: N(6)-methyladenosine modulates messenger RNA translation efficiency. Cell 161: 1388-1399, 2015.
36. Wang X, Lu Z, Gomez A, Hon GC, Yue Y, Han D, Fu Y, Parisien M, Dai Q, Jia G, *et al*: N6-methyladenosine-dependent regulation of messenger RNA stability. Nature 505: 117-120, 2014.
37. Schwartz S, Mumbach MR, Jovanovic M, Wang T, Maciag K, Bushkin GG, Mertins P, Ter-Ovanesyan D, Habib N, Cacchiarelli D, *et al*: Perturbation of m6A writers reveals two distinct classes of mRNA methylation at internal and 5' sites. Cell Rep 8: 284-296, 2014.
38. Wang P, Doxtader KA and Nam Y: Structural basis for cooperative function of Mettl3 and Mettl14 methyltransferases. Mol Cell 63: 306-317, 2016.
39. Jia G, Fu Y, Zhao X, Dai Q, Zheng G, Yang Y, Yi C, Lindahl T, Pan T, Yang YG and He C: N6-methyladenosine in nuclear RNA is a major substrate of the obesity-associated FTO. Nat Chem Biol 7: 885-887, 2011.
40. Zheng G, Dahl JA, Niu Y, Fedorcsak P, Huang CM, Li CJ, Vågbø CB, Shi Y, Wang WL, Song SH, *et al*: ALKBH5 is a mammalian RNA demethylase that impacts RNA metabolism and mouse fertility. Mol Cell 49: 18-29, 2013.
41. Shi H, Wei J and He C: Where, when, and how: Context-dependent functions of RNA methylation writers, readers, and erasers. Mol Cell 74: 640-650, 2019.
42. Xu K, Yang Y, Feng GH, Sun BF, Chen JQ, Li YF, Chen YS, Zhang XX, Wang CX, Jiang LY, *et al*: Mettl3-mediated m^6A regulates spermatogonial differentiation and meiosis initiation. Cell Res 27: 1100-1114, 2017.
43. Lin Z, Hsu PJ, Xing X, Fang J, Lu Z, Zou Q, Zhang KJ, Zhang X, Zhou Y, Zhang T, *et al*: Mettl3-/Mettl14-mediated mRNA N^6-methyladenosine modulates murine spermatogenesis. Cell Res 27: 1216-1230, 2017.
44. Wu Y, Xie L, Wang M, Xiong Q, Guo Y, Liang Y, Li J, Sheng R, Deng P, Wang Y, *et al*: Mettl3-mediated m^6A RNA methylation regulates the fate of bone marrow mesenchymal stem cells and osteoporosis. Nat Commun 9: 4772, 2018.
45. Tian C, Huang Y, Li Q, Feng Z and Xu Q: Mettl3 regulates osteogenic differentiation and alternative splicing of vegfa in bone marrow mesenchymal stem cells. Int J Mol Sci 20: 551, 2019.
46. Zhang Y, Gu X, Li D, Cai L and Xu Q: METTL3 regulates osteoblast differentiation and inflammatory response via smad signaling and MAPK signaling. Int J Mol Sci 21: 199, 2019.
47. Song H, Song J, Cheng M, Zheng M, Wang T, Tian S, Flavell RA, Zhu S, Li HB, Ding C, *et al*: METTL3-mediated m^6A RNA methylation promotes the anti-tumour immunity of natural killer cells. Nat Commun 12: 5522, 2021.
48. Huang M, Xu S, Liu L, Zhang M, Guo J, Yuan Y, Xu J, Chen X and Zou J: m6A methylation regulates osteoblastic differentiation and bone remodeling. Front Cell Dev Biol 9: 783322, 2021.
49. Nachbur U, Stafford CA, Bankovacki A, Zhan Y, Lindqvist LM, Fiil BK, Khakham Y, Ko HJ, Sandow JJ, Falk H, *et al*: A RIPK2 inhibitor delays NOD signalling events yet prevents inflammatory cytokine production. Nat Commun 6: 6442, 2015.
50. Tan X, Wei LJ, Fan GJ, Jiang YN and Yu XP: Effector responses of bovine blood neutrophils against Escherichia coli: Role of NOD1/NF-κB signalling pathway. Vet Immunol Immunopathol 168: 68-76, 2015.
51. Livak KJ and Schmittgen TD: Analysis of relative gene expression data using real-time quantitative PCR and the 2(-Delta Delta C(T)) method. Methods 25: 402-408, 2001.
52. Nguyen TTT, Shang E, Shu C, Kim S, Mela A, Humala N, Mahajan A, Yang HW, Akman HO, Quinzii CM, *et al*: Aurora kinase A inhibition reverses the Warburg effect and elicits unique metabolic vulnerabilities in glioblastoma. Nat Commun 12: 5203, 2021.
53. Li D, Yang J, Malik V, Huang Y, Huang X, Zhou H and Wang J: An RNAi screen of RNA helicases identifies eIF4A3 as a regulator of embryonic stem cell identity. Nucleic Acids Res 50: 12462-12479, 2022.
54. Ratnadiwakara M and Änkö ML: mRNA Stability assay using transcription inhibition by actinomycin D in mouse pluripotent stem cells. Bio Protoc 8: e3072, 2018.
55. Zhou Z, Cao Y, Yang Y, Wang S and Chen F: METTL3-mediated m^6A modification of lnc KCNQ1OT1 promotes doxorubicin resistance in breast cancer by regulating miR-103a-3p/MDR1 axis. Epigenetics 18: 2217033, 2023.
56. Luo S, Liao C, Zhang L, Ling C, Zhang X, Xie P, Su G, Chen Z, Zhang L, Lai T and Tang J: METTL3-mediated m6A mRNA methylation regulates neutrophil activation through targeting TLR4 signaling. Cell Rep 42: 112259, 2023.
57. Kim JM, Lin C, Stavre Z, Greenblatt MB and Shim JH: Osteoblast-osteoclast communication and bone homeostasis. Cells 9: 2073, 2020.
58. Redlich K and Smolen JS: Inflammatory bone loss: Pathogenesis and therapeutic intervention. Nat Rev Drug Discov 11: 234-250, 2012.
59. Li Y, Ling J and Jiang Q: Inflammasomes in alveolar bone loss. Front Immunol 12: 691013, 2021.
60. Jiang Y, Jia T, Gong W, Wooley PH and Yang SY: Titanium particle-challenged osteoblasts promote osteoclastogenesis and osteolysis in a murine model of periprosthestic osteolysis. Acta Biomater 9: 7564-7572, 2013.
61. Luo J, Xu T and Sun K: N6-methyladenosine RNA modification in inflammation: Roles, mechanisms, and applications. Front Cell Dev Biol 9: 670711, 2021.
62. Wu M, Chen G and Li YP: TGF-β and BMP signaling in osteoblast, skeletal development, and bone formation, homeostasis and disease. Bone Res 4: 16009, 2016.

63. Afzal F, Pratap J, Ito K, Ito Y, Stein JL, van Wijnen AJ, Stein GS, Lian JB and Javed A: Smad function and intranuclear targeting share a Runx2 motif required for osteogenic lineage induction and BMP2 responsive transcription. J Cell Physiol 204: 63-72, 2005.
64. Yan X, Liu Z and Chen Y: Regulation of TGF-beta signaling by Smad7. Acta Biochim Biophys Sin (Shanghai) 41: 263-272, 2009.
65. Deng Z, Zhang R, Li M, Wang S, Fu G, Jin J, Wang Z, Ma Y and Zheng Q: STAT3/IL-6 dependent induction of inflammatory response in osteoblast and osteoclast formation in nanoscale wear particle-induced aseptic prosthesis loosening. Biomater Sci 9: 1291-1300, 2021.
66. Cai Y, Yu R, Kong Y, Feng Z and Xu Q: METTL3 regulates LPS-induced inflammatory response via the NOD1 signaling pathway. Cell Signal 93: 110283, 2022.
67. Caruso R, Warner N, Inohara N and Núñez G: NOD1 and NOD2: Signaling, host defense, and inflammatory disease. Immunity 41: 898-908, 2014.
68. Pei G and Dorhoi A: NOD-like receptors: Guards of cellular homeostasis perturbation during infection. Int J Mol Sci 22: 6714, 2021.
69. Kersse K, Bertrand MJ, Lamkanfi M and Vandenabeele P: NOD-like receptors and the innate immune system: Coping with danger, damage and death. Cytokine Growth Factor Rev 22: 257-276, 2011.
70. Yang Y, Hsu PJ, Chen YS and Yang YG: Dynamic transcriptomic m^6A decoration: Writers, erasers, readers and functions in RNA metabolism. Cell Res 28: 616-624, 2018.
71. Jiang X, Liu B, Nie Z, Duan L, Xiong Q, Jin Z, Yang C and Chen Y: The role of m6A modification in the biological functions and diseases. Signal Transduct Target Ther 6: 74, 2021.
72. Du H, Zhao Y, He J, Zhang Y, Xi H, Liu M, Ma J and Wu L: YTHDF2 destabilizes m(6)A-containing RNA through direct recruitment of the CCR4-NOT deadenylase complex. Nat Commun 7: 12626, 2016.
73. Zhou J, Wan J, Gao X, Zhang X, Jaffrey SR and Qian SB: Dynamic m(6)A mRNA methylation directs translational control of heat shock response. Nature 526: 591-594, 2015.
74. Winkler R, Gillis E, Lasman L, Safra M, Geula S, Soyris C, Nachshon A, Tai-Schmiedel J, Friedman N, Le-Trilling VTK, *et al*: m^6A modification controls the innate immune response to infection by targeting type I interferons. Nat Immunol 20: 173-182, 2019.
75. Mapperley C, van de Lagemaat LN, Lawson H, Tavosanis A, Paris J, Campos J, Wotherspoon D, Durko J, Sarapuu A, Choe J, *et al*: The mRNA m6A reader YTHDF2 suppresses proinflammatory pathways and sustains hematopoietic stem cell function. J Exp Med 218: e20200829, 2021.
76. Fang C, He M, Li D and Xu Q: YTHDF2 mediates LPS-induced osteoclastogenesis and inflammatory response via the NF-κB and MAPK signaling pathways. Cell Signal 85: 110060, 2021.
77. Tsuchiya K, Yoshimura K, Inoue Y, Iwashita Y, Yamada H, Kawase A, Watanabe T, Tanahashi M, Ogawa H, Funai K, *et al*: YTHDF1 and YTHDF2 are associated with better patient survival and an inflamed tumor-immune microenvironment in non-small-cell lung cancer. Oncoimmunology 10: 1962656, 2021.
78. Wu R, Liu Y, Zhao Y, Bi Z, Yao Y, Liu Q, Wang F, Wang Y and Wang X: m^6A methylation controls pluripotency of porcine induced pluripotent stem cells by targeting SOCS3/JAK2/STAT3 pathway in a YTHDF1/YTHDF2-orchestrated manner. Cell Death Dis 10: 171, 2019.
79. Hsu PJ, Zhu Y, Ma H, Guo Y, Shi X, Liu Y, Qi M, Lu Z, Shi H, Wang J, *et al*: Ythdc2 is an N^6-methyladenosine binding protein that regulates mammalian spermatogenesis. Cell Res 27: 1115-1127, 2017.
80. Keegan GM, Learmonth ID and Case CP: Orthopaedic metals and their potential toxicity in the arthroplasty patient: A review of current knowledge and future strategies. J Bone Joint Surg Br 89: 567-573, 2007.
81. Gornet MF, Singh V, Schranck FW, Skipor AK and Jacobs JJ: Serum metal concentrations in patients with titanium ceramic composite cervical disc replacements. Spine (Phila Pa 1976) 42: 366-371, 2017.
82. Day JS, Baxter RM, Ramsey ML, Morrey BF, Connor PM, Kurtz SM and Steinbeck MJ: Characterization of wear debris in total elbow arthroplasty. J Shoulder Elbow Surg 22: 924-931, 2013.
83. Chassot E, Irigaray JL, Terver S and Vanneuville G: Contamination by metallic elements released from joint prostheses. Med Eng Phys 26: 193-199, 2004.
84. Lukina E, Laka A, Kollerov M, Sampiev M, Mason P, Wagstaff P, Noordeen H, Yoon WW and Blunn G: Metal concentrations in the blood and tissues after implantation of titanium growth guidance sliding instrumentation. Spine J 16: 380-388, 2016.
85. Safioti LM, Kotsakis GA, Pozhitkov AE, Chung WO and Daubert DM: Increased levels of dissolved titanium are associated with peri-implantitis-a cross-sectional study. J Periodontol 88: 436-442, 2017.
86. Zeng C, Huang W, Li Y and Weng H: Roles of METTL3 in cancer: Mechanisms and therapeutic targeting. J Hematol Oncol 13: 117, 2020.